hypomethylated IG-DMR directly controls the imprinting pattern of both *PEGs* and *MEGs*. These notions also explain the epigenotypic alteration in the previous cases with epimutations or microdeletions affecting both DMRs (Figure S3).

It remains to be clarified how the IG-DMR and the *MEG3*-DMR interact hierarchically in the body. However, the present data, together with the previous findings in cases with epimutations [2,5–8], imply that *MEG3*-DMR can remain hypomethylated only in the presence of a hypomethylated IG-DMR and is methylated when the IG-DMR is deleted or methylated irrespective of the parental origin. Furthermore, mouse studies have suggested that the methylation pattern of the postfertilization-derived *Gtl2*-DMR (the mouse homolog for the *MEG3*-DMR) is dependent on that of the germline-derive IG-DMR [18]. Thus, a preferential binding of some factor(s) to the unmethylated IG-DMR may cause a conformational alteration of the genomic structure, thereby protecting the methylation of the *MEG3*-DMR.

It also remains to be elucidated how the IG-DMR and the *MEG3*-DMR regulate the expression of both *PEGs* and *MEGs* in the placenta and the body, respectively. For the *MEG3*-DMR, however, the CTCF binding sites C and D may play a pivotal role in the imprinting regulation. The methylation analysis indicates that the two sites reside within the *MEG3*-DMR, and it is known that the CTCF protein with versatile functions preferentially binds to unmethylated target sequences including the sites C and D [11,19–21]. In this regard, all the *MEGs* in this imprinted region can be transcribed together in the same orientation and show a strikingly similar tissue expressions pattern [1,17], whereas *PEGs* are transcribed in different directions and are co-expressed with *MEGs* only in limited cell-types [1,22]. It is possible, therefore, that preferential CTCF binding to the grossly unmethylated sites C and D activates all the *MEGs* as a large transcription unit and represses all the *PEGs* perhaps by influencing chromatin structure and histone modification independently of the effects of expressed *MEGs*. In support of this, CTCF protein acts as a transcriptional activator for *Gtl2* (the mouse homolog for *MEG3*) in the mouse [23].

Such an imprinting control model has not been proposed previously. It is different from the CTCF protein-mediated insulator model indicated for the *H19*-DMR and from the non-coding RNA-mediated model implicated for several imprinted regions including the

KvDMR1 [24]. However, the KvDMR1 harbors two putative CTCF binding sites that may mediate non-coding RNA independent imprinting regulation [25], and the imprinting control center for Prader-Willi syndrome [26] also carries three CTCF binding sites (examined with a Search for CTCF DNA Binding Sites program, http://www.essex.ac.uk/bs/molonc/spa.html). Thus, while each imprinted region would be regulated by a different mechanism, a CTCF protein may be involved in the imprinting control of multiple regions, in various manners.

This imprinted region has also been studied in the mouse. Clinical and molecular findings in wildtype mice [1,27,28], mice with PatDi(12) (paternal disomy for chromosome 12 harboring this imprinted region) [18,29,30], and mice with targeted deletions for the IG-DMR (ΔIG-DMR) [12,27] and for the *Gtl2*-DMR (Δ*Gtl2*-DMR) [31] are summarized in Table 2. These data, together with human data, provide several informative findings. First, in both the human and the mouse, the IG-DMR is differentially methylated in both the body and the placenta, whereas the *MEG3/Gtl2*-DMR is differentially methylated in the body and exhibits non-DMR in the placenta. Second, the IG-DMR and the *MEG3/Gtl2*-DMR show a hierarchical interaction on the maternally derived chromosome in both the human and the mouse bodies. Indeed, the *MEG3/Gtl2*-DMR is epimutated in patient 1 and mice with maternally inherited ΔIG-DMR, and the IG-DMR is normally methylated in patient 2 and mice with maternally inherited Δ*Gtl2*-DMR. Third, the function of the IG-DMR is comparable between human and mouse bodies and different between human and mouse placentas. Indeed, patient 1 has upd(14)pat body and placental phenotypes, whereas mice with the ΔIG-DMR of maternal origin have PatDi(12)-compatible body phenotype and apparently normal placental phenotype. It is likely that imprinting regulation in the mouse placenta is contributed by some mechanism(s) other than the methylation pattern of the IG-DMR, such as chromatin conformation [27,32,33].

Unfortunately, however, the data of Δ*Gtl2*-DMR mice appears to be drastically complicated by the retained neomycin cassette in the upstream region of *Gtl2*. Indeed, it has been shown that the insertion of a *lacZ* gene or a neomycin gene in the similar upstream region of *Gtl2* causes severely dysregulated expression patterns and abnormal phenotypes after both paternal and maternal transmissions [34,35], and that deletion of the inserted neomycin gene results in apparently normal expression patterns and phenotypes after both paternal and

maternal transmissions [35]. (In this regard, although a possible influence of the inserted 66 bp segment can not be excluded formally in patient 2, phenotype and expression data in patient 2 are compatible with simple paternalization of the imprinted region.) In addition, since the apparently normal phenotype in mice homozygous for Δ*Gtl2*-DMR is reminiscent of that in sheep homozygous for the callipyge mutation [36], a complicated mechanism(s) such as the polar overdominance may be operating in the Δ*Gtl2*-DMR mice [37]. Thus, it remains to be clarified whether the *MEG3/Gtl2*-DMR has a similar or different function between the human and the mouse.

Two points should be made in reference to the present study. First, the proposed functions of the two DMRs are based on the results of single patients. This must be kept in mind, because there might be a hidden patient-specific abnormality or event that might explain the results. For example, the abnormal placental phenotype in patient 1 might be caused by some co-incidental aberration, and the apparently normal placenta in patient 2 might be due to mosaicism with grossly preserved *MEG3*-DMR in the placenta and grossly deleted *MEG3*-DMR in the body. Second, the clinical features in the mother of patient 1 such as short stature and obesity are often observed in cases with upd(14)mat (Table S2). However, the clinical features are non-specific and appear to be irrelevant to the microdeletion involving the IG-DMR, because loss of the paternally derived IG-DMR does not affect the imprinted status [2,12]. Indeed, *MEG3* in the mother of patient 1 showed normal monoallelic expression in the presence of the differentially methylated *MEG3*-DMR. Nevertheless, since the upd(14)mat phenotype is primarily ascribed to loss of functional *DLK1* (Figure S3B) [2,38], it might be possible that the microdeletion involving the IG-DMR has affected a *cis*-acting regulatory element for *DLK1* expression (for details, see Note in the legend for Table S2). Further studies in cases with similar microdeletions will permit clarification of these two points.

In summary, the results show a hierarchical interaction and distinct functional properties of the IG-DMR and the *MEG3*-DMR in imprinting control. Thus, this study provides significant advance in the clarification of mechanisms involved in the imprinting regulation at the 14q32.2 imprinted region and the development of upd(14) phenotype.

Methods

Ethics Statement

This study was approved by the Institutional Review Board Committees at National Center for Child health and Development, University College Dublin, and Dokkyo University School of Medicine, and performed after obtaining written informed consent.

Primers

All the primers utilized in this study are summarized in Table S3.

Sample preparation

For leukocytes and skin fibroblasts, genomic DNA (gDNA) samples were extracted with FlexiGene DNA Kit (Qiagen), and RNA samples were prepared with RNeasy Plus Mini (Qiagen) for *DLK1, MEG3, RTL1*, *MEG8* and *snoRNAs*, and with mirVana™ miRNA Isolation Kit (Ambion) for *microRNAs*. For paraffin-embedded tissues including the placenta, brain, lung, heart, liver, spleen, kidney, bladder, and small intestine, gDNA and RNA samples were extracted with RecoverAll™ Total Nucleic Acids Isolation Kit (Ambion) using slices of 40 μm thick. For fresh control placental samples, gDNA and RNA were extracted using ISOGEN (Nippon Gene). After treating total RNA samples with DNase, cDNA samples for *DLK1, MEG3, MEG8*, and *snoRNAs* were prepared with oligo(dT) primers from 1 μg of RNA using Superscript III Reverse Transcriptase (Invitrogen), and those for *microRNAs* were synthesized from 300 ng of RNA using TaqMan MicroRNA Reverse Transcription Kit (Applied Biosystems). For *RTL1*, cDNA samples were synthesized with *RTL1*-specific primers that do not amplify *RTL1as*. Control gDNA and cDNA samples were extracted from adult leukocytes and neonatal skin fibroblasts purchased from Takara Bio Inc. Japan, and from a fresh placenta of 38 weeks of gestation. Metaphase spreads were prepared from leukocytes and skin fibroblasts using colcemide (Invitrogen).

Structural analysis

Microsatellite analysis and SNP genotyping were performed as described previously [2].

For FISH analysis, metaphase spreads were hybridized with a 5,104 bp FISH-1 probe and a 5,182 bp FISH-2 probe produced by long PCR, together with an RP11-566I2 probe for 14q12 used as an internal control [2]. The FISH-1 and FISH-2 probes were labeled with digoxigenin and detected by rhodamine anti-digoxigenin, and the RP11-566I2 probe was labeled with biotin and detected by avidin conjugated to fluorescein isothiocyanate. For quantitative real-time PCR analysis, the relative copy number to RNaseP (catalog No: 4316831, Applied Biosystems) was determined by the Taqman real-time PCR method using the probe-primer mix on an ABI PRISM 7000 (Applied Biosystems). To determine the breakpoints of microdeletions, sequence analysis was performed for long PCR products harboring the fusion points, using serial forward primers on the CEQ 8000 autosequencer (Beckman Coulter). Direct sequencing was also performed on the CEQ 8000 autosequencer. Oligoarray comparative genomic hybridization was performed with 1x244K Human Genome Array (catalog No: G4411B) (Agilent Technologies), according to the manufacturer's protocol.

Methylation analysis

Methylation analysis was performed for gDNA treated with bisulfite using the EZ DNA Methylation Kit (Zymo Research). After PCR amplification using primer sets that hybridize both methylated and unmethylated clones because of lack of CpG dinucleotides within the primer sequences, the PCR products were digested with appropriate restriction enzymes for combined bisulfite restriction analysis. For bisulfite sequencing, the PCR products were subcloned with TOPO TA Cloning Kit (Invitrogen) and subjected to direct sequencing on the CEQ 8000 autosequencer.

Expression analysis

Standard RT-PCR was performed for *DLK1*, *RTL1*, *MEG3*, *MEG8*, and *snoRNAs* using primers hybridizing to exonic or transcribed sequences, and one μl of PCR reaction solutions was loaded onto Gel-Dye Mix (Agilent). Taqman real-time PCR was carried out using the probe-primer mixtures (assay No: Hs00292028 for *MEG3* and Hs00419701 for *MEG8*; assay ID: 001028 for *miR433*, 000452 for *miR127*, 000568 for *miR379*, and 000477 for *miR154*) on

the ABI PRISM 7000. Data were normalized against *GAPDH* (catalog No: 4326317E) for *MEG3* and *MEG8* and against *RNU48* (assay ID: 0010006) for the remaining *miRs*. The expression studies were performed three times for each sample.

To examine the imprinting status of *MEG3* in the leukocytes of the mother of patient 1, direct sequence data for informative cSNPs were compared between gDNA and cDNA. To analyze the imprinting status of *RTL1* in the placental sample of patient 1 and that of *DLK1* in the pituitary and adrenal samples of patient 2, RT-PCR products containing exonic cSNPs informative for the parental origin were subcloned with TOPO TA Cloning Kit, and multiple clones were subjected to direct sequencing on the CEQ 8000 autosequencer. Furthermore, *MEG3* expression pattern was examined using leukocyte gDNA and cDNA samples from multiple normal subjects and leukocyte gDNA samples from their mothers, and *RTL1* expression pattern was analyzed using gDNA and cDNA samples from multiple fresh normal placentas and leukocyte gDNA from the mothers.

Acknowledgments

This work was supported by grants from the Ministry of Health, Labor, and Welfare, from the Ministry of Education, Science, Sports and Culture, and from Takeda Science Foundation.

Author Contributions

Conceived and designed the experiments: MK ACF-S TO. Performed the experiments: MK MF KM FK. Contributed reagents/materials/analysis tool: MJO AJG YW OA NM KM TO. Wrote the paper: TO.

Competing Interests

The authors have declared that no competing interests exist.

References

1. da Rocha ST, Edwards CA, Ito M, Ogata T, Ferguson-Smith AC (2008) Genomic imprinting at the mammalian Dlk1-Dio3 domain. Trends Genet 24: 306–316.
2. Kagami M, Sekita Y, Nishimura G, Irie M, Kato F, et al. (2008) Deletions and epimutations affecting the human 14q32.2 imprinted region in individuals with paternal and maternal upd(14)-like phenotypes. Nat Genet 40: 237–242.
3. Kagami M, Yamazawa K, Matsubara K, Matsuo N, Ogata T (2008) Placentomegaly in paternal uniparental disomy for human chromosome 14. Placenta 29: 760–761.
4. Kotzot D (2004) Maternal uniparental disomy 14 dissection of the phenotype with respect to rare autosomal recessively inherited traits, trisomy mosaicism, and genomic imprinting. Ann Genet 47: 251–260.
5. Temple IK, Shrubb V, Lever M, Bullman H, Mackay DJ (2007) Isolated imprinting mutation of the DLK1/GTL2 locus associated with a clinical presentation of maternal uniparental disomy of chromosome 14. J Med Genet 44: 637–640.
6. Buiting K, Kanber D, Martín-Subero JI, Lieb W, Terhal P, et al. (2008) Clinical features of maternal uniparental disomy 14 in patients with an epimutation and a deletion of the imprinted DLK1/GTL2 gene cluster. Hum Mutat 29: 1141–1146.
7. Hosoki K, Ogata T, Kagami M, Tanaka T, Saitoh S (2008) Epimutation (hypomethylation) affecting the chromosome 14q32.2 imprinted region in a girl with upd(14)mat-like phenotype. Eur J Hum Genet 16: 1019–1023.
8. Zechner U, Kohlschmidt N, Rittner G., Damatova N, Beyer V, et al. (2009) Epimutation at human chromosome 14q32.2 in a boy with a upd(14)mat-like clinical phenotype. Clin Genet 75: 251–258.
9. Li E, Beard C, Jaenisch R (1993) Role for DNA methylation in genomic imprinting. Nature 366: 362–365.
10. Tsai CE, Lin SP, Ito M, Takagi N, Takada S, et al. (2002) Genomic imprinting contributes to thyroid hormone metabolism in the mouse embryo. Curr Biol 12: 1221–1226.
11. Rosa AL, Wu YQ, Kwabi-Addo B, Coveler KJ, Reid Sutton V, et al. (2005)

Allele-specific methylation of a functional CTCF binding site upstream of MEG3 in the human imprinted domain of 14q32. Chromosome Res 13: 809–818.

12. Lin SP, Youngson N, Takada S, Seitz H, Reik W, et al. (2003) Asymmetric regulation of imprinting on the maternal and paternal chromosomes at the Dlk1-Gtl2 imprinted cluster on mouse chromosome 12. Nat Genet 35: 97–102.
13. Sekita Y, Wagatsuma H, Nakamura K, Ono R, Kagami M, et al. (2008) Role of retrotransposon-derived imprinted gene, Rtl1, in the feto-maternal interface of mouse placenta. Nat Genet 40: 243–248.
14. Seitz H, Youngson N, Lin SP, Dalbert S, Paulsen M, et al. (2003) Imprinted microRNA genes transcribed antisense to a reciprocally imprinted retrotransposon-like gene. Nat Genet 34: 261–262.
15. Davis E, Caiment F, Tordoir X, Cavaillé J, Ferguson-Smith A, et al. (2005) RNAi-mediated allelic trans-interaction at the imprinted Rtl1/Peg11 locus. Curr Biol 15: 743–749.
16. Wylie AA, Murphy SK, Orton TC, Jirtle RL (2000) Novel imprinted DLK1/GTL2 domain on human chromosome 14 contains motifs that mimic those implicated in IGF2/H19 regulation. Genome Res 10: 1711–1718.
17. Tierling S, Dalbert S, Schoppenhorst S, Tsai CE, Oliger S, et al. (2007) High-resolution map and imprinting analysis of the Gtl2-Dnchc1 domain on mouse chromosome 12. Genomics 87: 225–235.
18. Takada S, Paulsen M, Tevendale M, Tsai CE, Kelsey G, et al. (2002) Epigenetic analysis of the Dlk1-Gtl2 imprinted domain on mouse chromosome 12: implications for imprinting control from comparison with Igf2-H19. Hum Mol Genet 11: 77–86.
19. Ohlsson R, Renkawitz R, Lobanenkov V (2001) CTCF is a uniquely versatile transcription regulator linked to epigenetics and disease. Trends Genet 17: 520–527.
20. Hark AT, Schoenherr CJ, Katz DJ, Ingram RS, Levorse JM, et al. (2000) CTCF mediates methylation-sensitive enhancer-blocking activity at the H19/Igf2 locus. Nature 405: 486–489.
21. Kanduri C, Pant V, Loukinov D, Pugacheva E, Qi CF, et al. (2000) Functional association of CTCF with the insulator upstream of the H19 gene is parent of origin-specific and

methylation-sensitive. Curr Biol 10: 853–856.

22. da Rocha ST, Tevendale M, Knowles E, Takada S, Watkins M, et al. (2007) Restricted co-expression of Dlk1 and the reciprocally imprinted non-coding RNA, Gtl2: implications for cis-acting control. Dev Biol 306: 810–823.
23. Wan LB, Pan H, Hannenhalli S, Cheng Y, Ma J, et al. (2008) Maternal depletion of CTCF reveals multiple functions during oocyte and preimplantation embryo development. Development 135: 2729–2738.
24. Ideraabdullah FY, Vigneau S, Bartolomei MS (2008) Genomic imprinting mechanisms in mammals. Mutat Res 647: 77–85.
25. Fitzpatrick GV, Pugacheva EM, Shin JY, Abdullaev Z, Yang Y, et al. (2007) Allele-specific binding of CTCF to the multipartite imprinting control region KvDMR1. Mol Cell Biol 27: 2636–2647.
26. Horsthemke B, Wagstaff J (2008) Mechanisms of imprinting of the Prader-Willi/Angelman region. Am J Med Genet A 146A: 2041–2052.
27. Lin SP, Coan P, da Rocha ST, Seitz H, Cavaille J, et al. (2007) Differential regulation of imprinting in the murine embryo and placenta by the Dlk1-Dio3 imprinting control region. Development 134: 417–426.
28. Coan PM, Burton GJ, Ferguson-Smith AC (2005) Imprinted genes in the placenta--a review. Placenta 26 Suppl A: S10–20.
29. Georgiades P, Watkins M, Surani MA, Ferguson-Smith AC (2000) Parental origin-specific developmental defects in mice with uniparental disomy for chromosome 12. Development 127: 4719–4728.
30. Takada S, Tevendale M, Baker J, Georgiades P, Campbell E, et al. (2000) Delta-like and gtl2 are reciprocally expressed, differentially methylated linked imprinted genes on mouse chromosome 12. Curr Biol 10: 1135–1138.
31. Takahashi N, Okamoto A, Kobayashi R, Shirai M, Obata Y, et al. (2009) Deletion of Gtl2, imprinted non-coding RNA, with its differentially methylated region induces lethal parent-origin-dependent defects in mice. Hum Mol Genet 18: 1879–1888.
32. Lewis A, Mitsuya K, Umlauf D, Smith P, Dean W, et al. (2004) Imprinting on distal

chromosome 7 in the placenta involves repressive histone methylation independent of DNA methylation. Nat Genet 36: 1291–1295.

33. Umlauf D, Goto Y, Cao R, Cerqueira F, Wagschal A, et al. (2004) Imprinting along the Kcnq1 domain on mouse chromosome 7 involves repressive histone methylation and recruitment of Polycomb group complexes. Nat Genet 36: 1296–1300.
34. Sekita Y, Wagatsuma H, Irie M, Kobayashi S, Kohda T, et al. (2006) Aberrant regulation of imprinted gene expression in Gtl2lacZ mice. Cytogenet. Genome Res 113: 223–229.
35. Steshina EY, Carr MS, Glick EA, Yevtodiyenko A, Appelbe OK, et al. (2006) Loss of imprinting at the Dlk1-Gtl2 locus caused by insertional mutagenesis in the Gtl2 5' region. BMC Genet 7: 44.
36. Charlier C, Segers K, Karim L, Shay T, Gyapay G, et al. (2001) The callipyge mutation enhances the expression of coregulated imprinted genes in cis without affecting their imprinting status. Nat Genet 27: 367–369.
37. Georges M, Charlier C, Cockett N (2003) The callipyge locus: evidence for the trans interaction of reciprocally imprinted genes. Trends Genet 19: 248–252.
38. Moon YS, Smas CM, Lee K, Villena JA, Kim KH, et al. (2002) Mice lacking paternally expressed Pref-1/Dlk1 display growth retardation and accelerated adiposity. Mol Cell Biol 22: 5585–5592.

Figure Legends

Figure 1. Clinical phenotypes of patients 1 and 2 at birth.
Both patients have bell shaped thorax with coat hanger appearance of the ribs and omphalocele. In patient 1, histological examination of the placenta shows proliferation of dilated and congested chorionic villi, as has previously been observed in a case with upd(14)pat [2]. For comparison, the histological finding of a gestational age matched (33 weeks) control placenta is shown in a dashed square. The horizontal black bars indicate 100 μm.

Figure 2. Physical map of the 14q32.2 imprinted region and the deleted segments in patient 1 and her mother and in patient 2 (shaded in gray). *PEGs* are shown in blue, *MEGs* in red, and the IG-DMR (CG4 and CG6) and the *MEG3*-DMR (CG7) in green. It remains to be clarified whether *DIO3* is a *PEG*, although mouse *Dio3* is known to be preferentially but not exclusively expressed from a paternally derived chromosome [10]. For *MEG3*, the isoform 2 with nine exons (red bars) and eight introns (light red segment) is shown (Ensembl; http://www.ensembl.org/index.html). Electrochromatograms represent the fusion point in patient 1 and her mother, and the fusion point accompanied by insertion of a 66 bp segment (highlighted in blue) with a sequence identical to that within *MEG3* intron 5 (the blue bar) in patient 2. Since PCR amplification with primers flanking the 66 bp segment at *MEG3* intron 5 has produced a 194 bp single band in patient 2 as well as in a control subject (shown in the box), this indicates that the 66 bp segment at the fusion point is caused by a duplicated insertion rather than by a transfer from intron 5 to the fusion point (if the 66 bp is transferred from the original position, a 128 bp band as well as a 194 bp band should be present in patient 2) (the marker size: 100, 200, and 300 bp). In the FISH images, the red signals (arrows) have been identified by the FISH-1 probe and the FISH-2 probe, and the light green signals (arrowheads) by the RP11-566I2 probe for 14q12 used as an internal control. The faint signal detected by the FISH-2 probe in patient 2 is consistent with the preservation of a ~1.2 kb region identified by the centromeric portion of the FISH-2 probe.

Figure 3. Methylation analysis. Filled and open circles indicate methylated and unmethylated cytosines at the CpG dinucleotides, respectively.

(A) Structure of CG4 and CG6 (the IG-DMR) and CG7 (the *MEG3*-DMR), and sequence of the putative CTCF binding sites [11]. Pat: paternally derived chromosome; and Mat: maternally derived chromosome. The PCR products for CG4 (311 bp) harbor 6 CpG dinucleotides and a G/A SNP (*rs12437020*), and are digested with *Bst*UI into three fragment (33 bp, 18 bp, and 260 bp) when the cytosines at the first and the second CpG dinucleotides and the fourth and the fifth CpG dinucleotides (indicated with orange rectangles) are methylated. The PCR products for CG6 (428 bp) carry 19 CpG dinucleotides and a C/T SNP (*rs10133627*), and are digested with *Taq*I into two fragment (189 bp and 239 bp) when the cytosine at the 9th CpG dinucleotide (indicated with an orange rectangle) is methylated. The PCR products for CG7 harbor 7 CpG dinucleotides, and are digested with *Bst*UI into two fragment (56 bp and 112 bp) when the cytosines at the fourth and the fifth CpG dinucleotides (indicated with orange rectangles) are methylated. These enzymes have been utilized for combined bisulfite restriction analysis (COBRA). For the putative CTCF binding sites A–G, the consensus CTCF binding motifs are shown in red letters; the cytosine residues at the CpG dinucleotides within the CTCF binding motifs are highlighted in blue, and those outside the CTCF binding motifs are highlighted in green.

(B) Methylation analysis of CG4, CG6, and CG7. Left part shows bisulfite sequencing data. The SNP typing data are also denoted for CG4 and CG6. The circles highlighted in orange correspond to those shown in Figure 3A. The relatively long CG6 was not amplified from the formalin-fixed and paraffin-embedded placental samples, probably because of the degradation of genomic DNA. Note that CG4 is differentially methylated in a control placenta and is massively hypermethylated in a upd(14)pat placenta, whereas CG7 is rather hypomethylated in a upd(14)pat placenta as well as in a control placenta. Right part shows COBRA data. U: unmethylated clone specific bands (311 bp for CG4, 428 bp for CG6, and 168 bp for CG7); and M: methylated clone specific bands (260 bp for CG4, 239 bp and 189 bp for CG6, and 112 bp and 56 bp for CG7). The results reproduce the bisulfite sequencing data, and delineate normal findings of the father of patient 1 and the parents of patient 2.

(C) Methylation analysis of the putative CTCF protein binding sites A–G. Left part shows bisulfite sequencing data, using leukocyte genomic DNA samples. Since PCR products for the site B contain a C/A SNP (*rs11627993*), genotyping data are also indicated. The circles highlighted in blue correspond to those shown in Figure 3A. The sites C and D exhibit clear DMRs. Right part indicates the results of the sites C and D using leukocyte and/or placental genomic DNA samples. The findings are similar to those of CG7.

(D) Allele-specific methylation pattern of the CTCF binding site D. A novel G/A SNP has been identified in a single control subject, as shown on a reverse chromatogram delineating a C/T SNP pattern, while the previously reported three SNPs were present in a homozygous condition. Methylated and unmethylated clones are associated with the "G" and the "A" alleles, respectively.

Figure 4. Expression analysis.

(A) Reverse transcriptase (RT)-PCR analysis. L: leukocytes; SF: skin fibroblasts; and P: placenta. The relatively weak *GAPDH* expression for the formalin-fixed and paraffin-embedded placenta of patient 1 indicates considerable mRNA degradation. Since a single exon was amplified for *DLK1* and *RTL1*, PCR was performed with and without RT for the placenta of patient 1, to exclude the possibility of false positive results caused by genomic DNA contamination.

(B) Quantitative real-time PCR (q-PCR) analysis of *MEG3*, *MEG8*, and *miRNAs*, using fresh skin fibroblasts (SF) of patient 2 and four control neonates. Of the examined *MEGs*, *miR433* and *miR127* are encoded by *RTL1as*.

(C) RT-PCR analysis for the formalin-fixed and paraffin-embedded pituitary (Pit.) and the adrenal (Ad.) in patient 2. The bands for *DLK1* are detected in the presence of RT and undetected in the absence of RT, thereby excluding contamination of genomic DNA.

(D) Monoallelic *MEG3* expression in the leukocytes of the mother of patient 1. The three cSNPs are present in a heterozygous status in gDNA and in a hemizygous status in cDNA. D: direct sequence.

(E) Biparental *RTL1* expression in the placenta of patient 1 and biparental *DLK1* expression in

the pituitary and adrenal of patient 2. D: direct sequence; and S: subcloned sequence. In patient 1, genotyping of *RTL1* cSNP (*rs6575805*) using gDNA indicates maternal origin of the "C" allele and paternal origin of the "T" allele, and sequencing analysis using cDNA confirms expression of maternally as well as paternally derived *RTL1*. Similarly, in patient 2, genotyping of *DLK1* cSNP (*rs1802710*) using gDNA denotes maternal origin of the "C" allele and paternal origin of the "T" alleles, and sequencing analysis using cDNA confirms expression of maternally as well as paternally inherited *DLK1*.

Figure 5. Schematic representation of the observed and predicted methylation and expression patterns. Deleted regions in patients 1 and 2 and the mother of patient 1 are indicated by stippled rectangles. P: paternally derived chromosome; and M: maternally derived chromosome. Representative imprinted genes are shown; these genes are known to be imprinted in the body and the placenta [2] (see also Figure S2). Placental samples have not been obtained in patient 2 and the mother of patient 1 (highlighted with light green backgrounds). Thick arrows for *RTL1* in patients 1 and 2 represent increased *RTL1* expression that is ascribed to loss of functional microRNA-containing *RTL1as* as a repressor for *RTL1* [12–15]; this phenomenon has been indicated in placentas with upd(14)pat and in those with an epimutation and a microdeletion involving the two DMRs (Figure S3A and S3C) [2]. *MEG3* and *RTL1as* that are disrupted or predicted to have become silent on the maternally derived chromosome are written in gray. Filled and open circles represent hypermethylated and hypomethylated DMRs, respectively; since the *MEG3*-DMR is rather hypomethylated and regarded as non-DMR in the placenta [2] (see also Figure 3), it is painted in gray.

Table 1. Clinical Features in Patients 1 and 2.

	Patient 1	Patient 2	Upd(14)pat (n=20)[c]
Present age	5.5 months	Deceased at 4 days	0–9 years
Sex	Female	Female	Male:Female=9:11
Karyotype	46,XX	46,XX	
Pregnancy and delivery			
Gestational age (weeks)	33	28	28–37
Delivery	Caesarean	Vaginal	Vaginal:Caesarean=6:7
Polyhydramnios	Yes	No	20/20 (<28)[d]
Amnioreduction (weeks)	2x (28, 30)	No	6/6
Placentomegaly	Yes	No	10/10
Growth pattern			
Prenatal growth failure	No	No	1/13
Birth length (cm)	43 (WNR)[a]	34 (WNR)[a]	
Birth weight (kg)	2.84 (>90 centile)[a]	1.32 (WNR)[a]	
Postnatal growth failure	Yes	…	5/6
Present stature (cm)	56.3 (–3.0 SD)[b]	…	
Present weight (kg)	5.02 (–3.0 SD)[b]	…	
Characteristic face			
Frontal bossing	No	Yes	5/7
Hairy forehead	Yes	Yes	9/10
Blepharophimosis	Yes	No	14/15
Depressed nasal bridge	Yes	Yes	13/13
Anteverted nares	Yes	No	6/10
Small ears	Yes	Yes	11/12
Protruding philtrum	Yes	No	15/15
Puckered lips	No	No	3/10
Micrognathia	Yes	Yes	11/12
Thoracic abnormality			
Bell-shaped thorax	Yes	Yes	17/17
Mechanical ventilation	Yes	Yes	17/17
Abdominal wall defect			
Diastasis recti	…	…	15/17
Omphalocele	Yes	Yes	2/17[e]
Others			
Short webbed neck	Yes	Yes	14/14
Cardiac disease	No	Yes (PDA)	5/10
Inguinal hernia	No	No	2/6
Coxa valga	Yes	No	3/4
Joint contractures	Yes	No	8/10
Kyphoscoliosis	No	No	4/7
Extra features		Hydronephrosis (bilateral)	

WNR: within the normal range; SD: standard deviation; and PDA: patent ductus arteriosus.

[a] Assessed by the gestational age- and sex-matched Japanese reference data from the Ministry of Health, Labor, and Welfare (http://wwwdbtk.mhlw.go.jp/toukei/).

[b] Assessed by the age- and sex-matched Japanese reference data.

[c] In the column summarizing the clinical features of 20 patients with upd(14)pat, the denominators indicate the number of cases examined for the presence or absence of each feature, and the numerators represent the number of cases assessed to be positive for that feature; thus, the differences between the denominators and the numerators denote the number of cases evaluated to be negative for that feature (adopted from reference [2]).

[d] Polyhydramnios has been identified by 28 weeks of gestation.

[e] Omphalocele is present in two cases with upd(14)pat and in two cases with epimutations [2].

Table 2. Clinical and Molecular Findings in Wildtype and PatDi(12) Mice and Mice with Maternally Inherited ΔIG-DMR and Δ*Gtl2*-DMR.

	Wildtype	PatDi(12)	ΔIG-DMR (~4.15 kb)[a]	Δ*Gtl2*-DMR (~10 kb)[b] Neomycin cassette (+)
<Body>				
Phenotype	Normal	Abnormal[c]	PatDi(12) phenotype[c]	Normal at birth Lethal by 4 weeks
Methylation pattern				
IG-DMR	Differential	Methylated	Methylated[d]	Differential
Gtl2-DMR	Differential	Methylated	Epimutated[e]	Methylated[d]
Expression pattern				
Pegs	Monoallelic	Increased (~2x)	Biparental Increased (2x or 4.5x)[f]	Grossly normal
Megs	Monoallelic	Absent	Absent	Decreased (<0.2~0.5x)[g]
<Placenta>				
Phenotype	Normal	Placentomegaly	Apparently normal	Not determined
Methylation pattern				
IG-DMR	Differential	Methylated	Not determined	Not determined
Gtl2-DMR	Non-DMR	Non-DMR	Not determined	Not determined
Expression pattern				
Pegs	Monoallelic	Not determined	Increased (1.5~1.8x)[g]	Decreased (0.5~0.85x)[g]
Megs	Monoallelic	Not determined	Decreased (0.6~0.8x)[g]	Decreased (<0.1~1.0)[g]
Remark			Paternal transmission[h]	Paternal transmission[i] Biparental transmission[j]

[a] The deletion size is smaller than that of patient 1 and her mother in this study, especially at the centromeric region.

[b] The microdeletion also involves *Gtl2*, and the deletion size is larger than that of patient 2 in this study.

[c] Body phenotype includes bell-shaped thorax with rib anomalies, distended abdomen, and short and broad neck.

[d] Hemizygosity for the methylated DMR of paternal origin.

[e] Hypermethylation of the maternally derived DMR.

[f] 2x *Dlk1* and *Dio3* expression levels and 4.5x *Rtl1* expression level. The markedly elevated *Rtl1* expression level is ascribed to a synergic effect between activation of the usually silent *Rtl1* of maternal origin and loss of functional microRNA-containing *Rtl1as* as a repressor for *Rtl1* [12–15].

[g] The expression level is variable among examined tissues and examined genes.

[h] The ΔIG-DMR of paternal origin has permitted normal *Gtl2*-DMR methylation pattern, intact imprinting status, and normal phenotype in the body (no data on the placenta).

[i] The Δ*Gtl2*-DMR of paternal origin is accompanied by normal methylation pattern of the IG-DMR and variably reduced *Pegs* expression and increased *Megs* expression in the body, and has yielded severe growth retardation accompanied by perinatal lethality.

[j] The homozygous mutants have survived and developed into fertile adults, despite rather altered expression patterns of the imprinted genes.

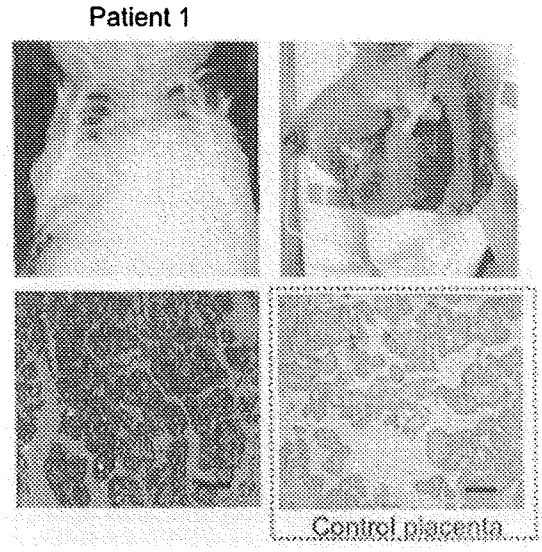
Patient 1
Control placenta
Patient 2

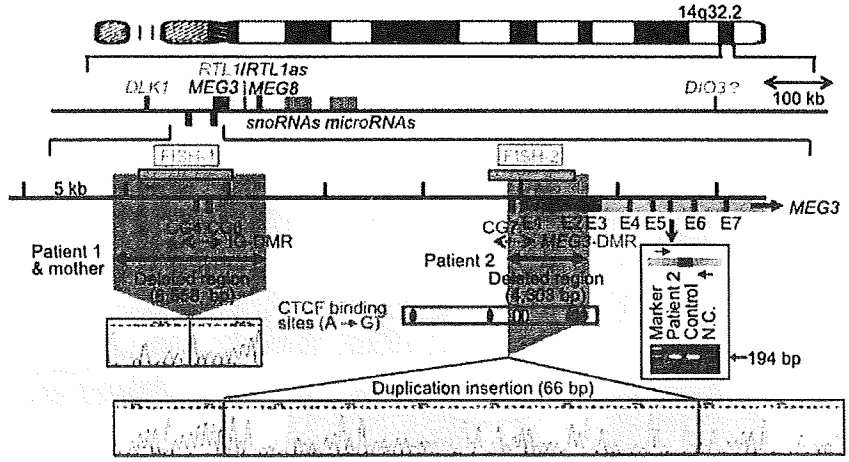
14q32.2
RTL1/RTL1as
DLK1
MEG3
MEG8
DIO3?
100 kb
snoRNAs microRNAs
FISH-1
FISH-2
5 kb
MEG3
E1 E2 E3 E4 E5 E6 E7
Patient 1
& mother
Patient 2
CTCF binding
sites (A→G)
Marker
Patient 2
Control
N.C.
194 bp
Duplication insertion (66 bp)

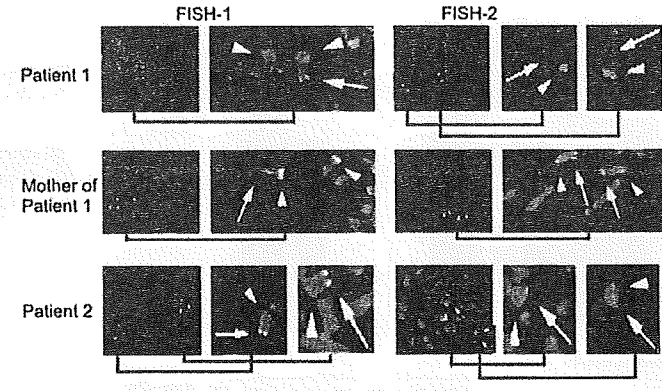
FISH-1
FISH-2
Patient 1
Mother of
Patient 1
Patient 2

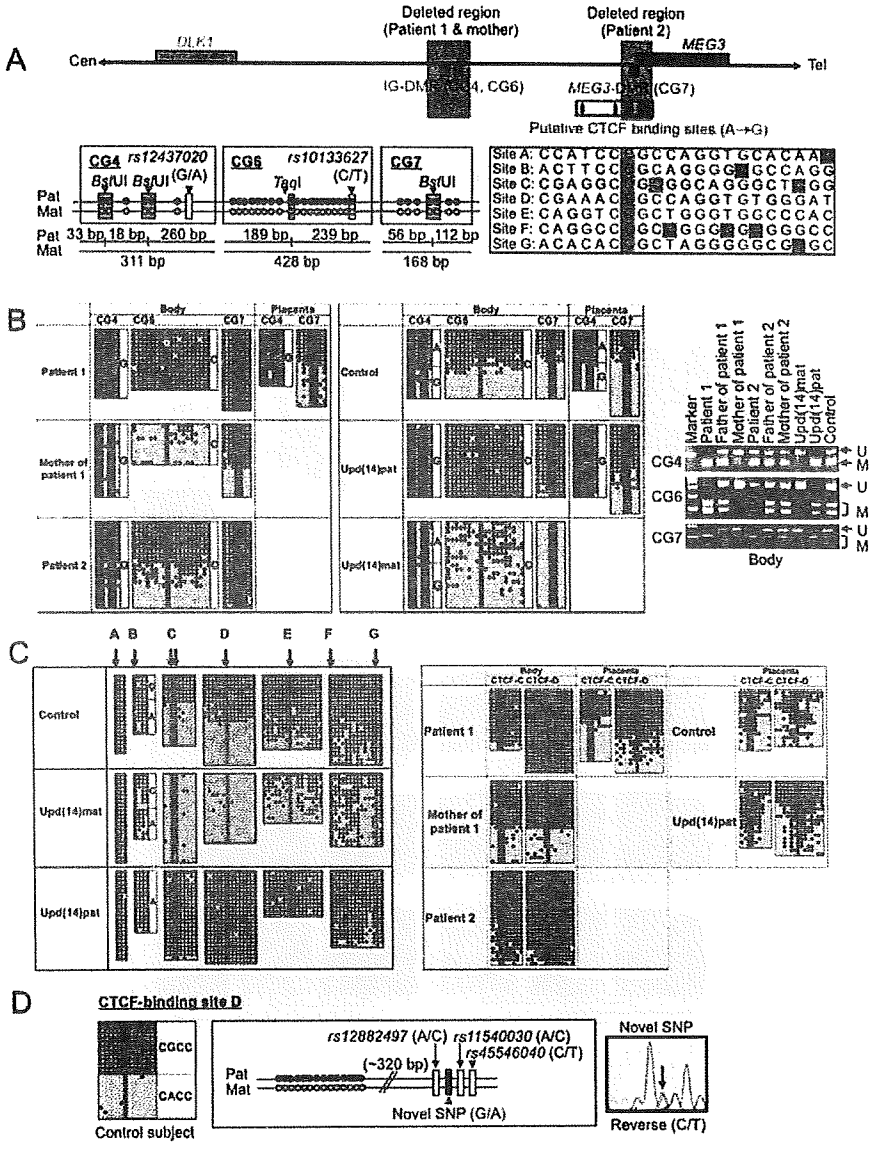
A
Deleted region (Patient 1 & mother)
Deleted region (Patient 2)
DLK1
MEG3
Cen
Tel
IG-DMR (CG4, CG6)
MEG3-DMR (CG7)
Putative CTCF binding sites (A→G)
CG4 rs12437020 BstUI BstUI (G/A)
CG6 rs10133627 TaqI (C/T)
CG7 BstUI
Pat
Mat
33 bp 18 bp 260 bp
189 bp 239 bp
56 bp 112 bp
311 bp
428 bp
168 bp
Site A: CCATCCGCCAGGTGCACAA
Site B: ACTTCCGCAGGGGCCAGG
Site C: CGAGGCGGGCAGGGCTGG
Site D: CGAAACGCCAGGTGTGGGAT
Site E: CAGGTGGCTGGGTGGCCCAC
Site F: CAGGCCGCGGCGGGGCC
Site G: ACACACGCTAGGGGGCGGC
B
Body
Placenta
CG4
CG6
CG7
Patient 1
Mother of patient 1
Patient 2
Control
Upd(14)pat
Upd(14)mat
Marker
Father of patient 1
Father of patient 2
Mother of patient 2
U
M
Body
C
A B C D E F G
Control
Upd(14)mat
Upd(14)pat
CTCF-C CTCF-D
Patient 1
Mother of patient 1
Patient 2
D
CTCF-binding site D
CGCC
CACC
Control subject
rs12882497 (A/C)
rs11540030 (A/C)
rs4546040 (C/T)
(~320 bp)
Pat
Mat
Novel SNP (G/A)
Novel SNP
Reverse (C/T)